Joint-Detection using Fast Fourier Transforms in TD-CDMA based Mobile Radio Systems

Marius Vollmer[1,2] *Jürgen Götze*[2] *Martin Haardt*[1]

1. Siemens AG, ICN CA CTO 7
Communication on Air
Hofmannstr. 51
D-81359 Munich, Germany
Martin.Haardt@icn.siemens.de
Marius.Vollmer@icn.siemens.de

2. Information Processing Lab
University of Dortmund
Otto-Hahn-Str. 4
D-44221 Dortmund, Germany
goetze@dt.e-technik.uni-dortmund.de
mvo@dt.e-technik.uni-dortmund.de

Abstract

Third generation mobile radio systems will employ TD-CDMA in their TDD mode. In a TD-CDMA mobile radio system, joint-detection is equivalent to solving a least squares problem with a block-Toeplitz system matrix. By extending this matrix to a block-circulant matrix, it is possible to block-diagonalize the matrix with Fast Fourier Transforms. For the typical system scenario of a TD-CDMA system, the circularization requires only a slight modification of the system matrix. In addition, overlap-save techniques can be employed to reduce the computational complexity even further. The resulting joint detection algorithm is able to produce better bit error ratios than the conventional algorithm that is based on an approximate Cholesky decomposition while requiring even less computational effort.

Keywords: TD-CDMA, joint detection, Toeplitz structure, Fast Fourier Transform, overlap save.

I. Introduction

In January 1998, the European standardization body for third generation mobile radio systems, the ETSI Special Mobile Group (SMG), has agreed on a radio access scheme for third generation mobile radio systems, called Universal Mobile Telecommunications System (UMTS). This agreement recommends the use of WCDMA (wideband CDMA) in the paired portion of the radio spectrum (FDD mode) and TD-CDMA (Time Division CDMA) in the unpaired portion (TDD mode). TD-CDMA is a burst structured system where multiple users are separated by spreading codes within one burst.

To overcome the near/far problem of traditional CDMA systems, receiver structures have been proposed for TD-CDMA that perform joint (or multi-user) detection [6]. A joint detector combines the knowledge about all users that share one burst into one large system of equations. This knowledge consists of the channel impulse responses that have been estimated from training sequences, the spreading codes, and the received antenna samples. The system of equations can be very large and thus algorithms must be developed to exploit its special structural characteristics, namely its band and block-Toeplitz structure. In [2] an approach based on the Cholesky algorithm was presented. The band structure of the system matrix leads to an approximate block-Toeplitz structure in the desired Cholesky factor. This has been ex-

ploited by computing the Cholesky factor of a smaller subproblem and using it to build the complete Cholesky factor from copies of that smaller factor [8]. In [9] the Schur algorithm was used to exploit the Toeplitz structure directly. This approach leads to a row-oriented technique for approximating the Cholesky factor.

In this paper a different route is taken in order to obtain the solution of the joint detection problem. The original block-Toeplitz system matrix is extended into a block-circulant matrix. This block-circulant matrix can then be inverted with little computational effort by using block-FFTs and overlap-save techniques.

The paper is organized as follows: Section II explains the data model used to derive the system equation; section III shows how block-circulant matrices can be diagonalized with block-FFTs; section IV applies this result to the TD-CDMA system; section V explains the overlap-save techniques; section VI presents simulation results and computational complexity figures for several joint detection algorithms.

II. Data Model

In the TD-CDMA system, K CDMA codes are simultaneously active on the same frequency and in the same time slot. The burst structure for this time-slotted CDMA concept is illustrated in figure 1. A burst consists of a guard interval that isolates it from the neighboring bursts and two data blocks (of N symbols each), separated by a user specific midamble that is used for channel estimation [2]. The receiver has K_a antennas. Before the received samples are used for the joint detection process, the influence of the midamble is removed. Therefore, we can restrict our discussion to one data block in the sequel, without loss of generality.

The mathematical description of the transmission system is based on the model depicted in figure 2. Since we are dealing with a burst structured system where individual data blocks are separated by a guard period, we can treat each block separately. Furthermore, it is assumed that the channel can be modeled by a FIR filter that is time-invariant during one burst. Likewise, each symbol will be spread with the same spreading code so that this spreading can also be modeled by a time-invariant convolution, combined with a suitable up-sampling of the data sequence.

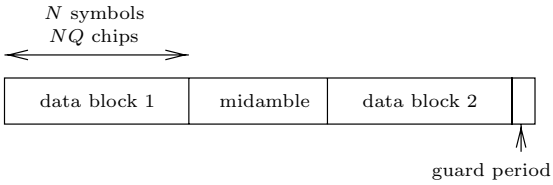

Figure 1: *The structure of one burst of the TD-CDMA system.*

The spreading factor is denoted by Q, the channel impulse response length is W, and K is the number of active users. The two convolutions can be combined into one with the impulse response vector

$$\boldsymbol{b}^{(k,k_a)} = \boldsymbol{c}^{(k)} \star \boldsymbol{h}^{(k,k_a)}$$

where $\boldsymbol{c}^{(k)} \in \mathbb{C}^Q$ is the spreading code of user k, $\boldsymbol{h}^{(k,k_a)} \in \mathbb{C}^W$ is the impulse response of the channel between the kth sender and the k_ath antenna, $\boldsymbol{b}^{(k,k_a)} \in \mathbb{C}^P$, $P = Q + W - 1$, $k = 1 \dots K$, and $k_a = 1 \dots K_a$. The $\star$ denotes the linear convolution of two finite sequences.

Let $\boldsymbol{d}^{(k)}$ be the data symbol sequence of user k and $\mathcal{S}_Q(\boldsymbol{d}^{(k)})$ denote the result of up-sampling $\boldsymbol{d}^{(k)}$ by a factor Q but without the last $Q-1$ zeros. Then we can express the vector of the received samples at antenna k_a as

$$\boldsymbol{e}^{(k_a)} = \sum_{k=1}^{K} \left(\boldsymbol{b}^{(k,k_a)} \star \mathcal{S}_Q(\boldsymbol{d}^{(k)}) \right) + \boldsymbol{n}^{(k_a)}, \quad (1)$$

$k_a = 1 \dots K_a$, where $\boldsymbol{n}^{(k_a)}$ represents the noise and intercell interference at the k_ath antenna. Since we drop the last $Q-1$ zeros after the up-sampling, we have $\boldsymbol{e}^{(k_a)} \in \mathbb{C}^{NQ+W-1}$. Likewise, $\boldsymbol{n}^{(k_a)} \in \mathbb{C}^{NQ+W-1}$. Here, N is the number of symbols in $\boldsymbol{d}^{(k)}$.

The data models (1) for all antennas can be combined into the matrix equation

$$\boldsymbol{e} = \boldsymbol{T}\boldsymbol{d} + \boldsymbol{n}, \quad (2)$$

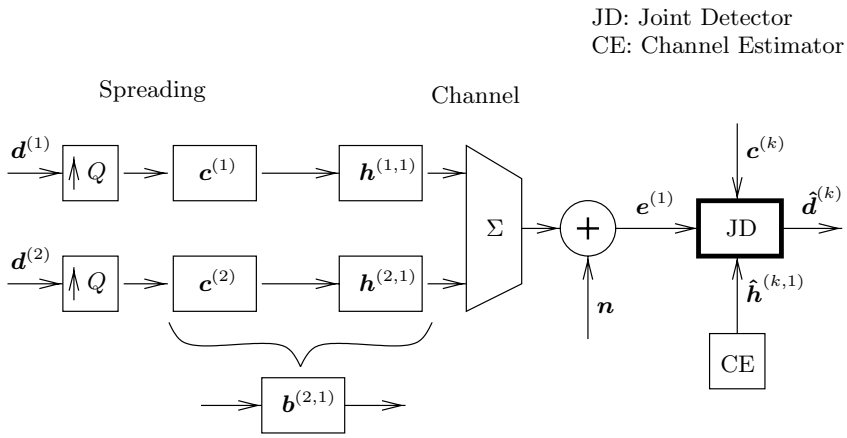

Figure 2: *Model of a CDMA transmission system for two users and one antenna.*

where the system matrix $\boldsymbol{T}$ contains suitable placed copies of all $\boldsymbol{b}^{(k,k_a)}$ and $\boldsymbol{d}$ is a suitable combination of all $\boldsymbol{d}^{(k)}$.

It is beneficial to arrange $\boldsymbol{T}$ in such a way that it has a *block-Sylvester* structure. This structure is depicted in figure 3. The matrix $\boldsymbol{V}$ in figure 3 is defined as

$$\boldsymbol{V} = \begin{bmatrix} \boldsymbol{b}^{(1)} & \boldsymbol{b}^{(2)} & \cdots & \boldsymbol{b}^{(K)} \end{bmatrix} \tag{3}$$

with

$$\boldsymbol{b}^{(k)} = \begin{bmatrix} \boldsymbol{b}_{(1,k)} & \boldsymbol{b}_{(2,k)} & \cdots & \boldsymbol{b}_{(P,k)} \end{bmatrix}^T \tag{4}$$

$$\boldsymbol{b}_{(p,k)} = \begin{bmatrix} b_p^{(k,1)} & b_p^{(k,2)} & \cdots & b_p^{(k,K_a)} \end{bmatrix}. \tag{5}$$

Likewise

$$\boldsymbol{e} = \begin{bmatrix} \boldsymbol{e}_{(1)} & \boldsymbol{e}_{(2)} & \cdots & \boldsymbol{e}_{(NQ+W-1)} \end{bmatrix}^T \tag{6}$$

$$\boldsymbol{e}_{(i)} = \begin{bmatrix} e_i^{(1)} & e_i^{(2)} & \cdots & e_i^{(K_a)} \end{bmatrix}. \tag{7}$$

The combined noise vector $\boldsymbol{n}$ is constructed from $\boldsymbol{n}^{(k_a)}$ in a similar form.
This leads to the following arrangement of the vector $\boldsymbol{d}$:

$$\boldsymbol{d} = \begin{bmatrix} \boldsymbol{d}_{(1)} & \boldsymbol{d}_{(2)} & \cdots & \boldsymbol{d}_{(N)} \end{bmatrix}^T \tag{8}$$

where $\boldsymbol{d}_{(i)}$ is a vector containing the ith symbol of all users:

$$\boldsymbol{d}_{(i)} = \begin{bmatrix} d_i^{(1)} & d_i^{(2)} & \cdots & d_i^{(K)} \end{bmatrix}. \tag{9}$$

In the sequel, we assume $K_a = 1$, but the derivation can be easily adapted to receivers with multiple antennas.

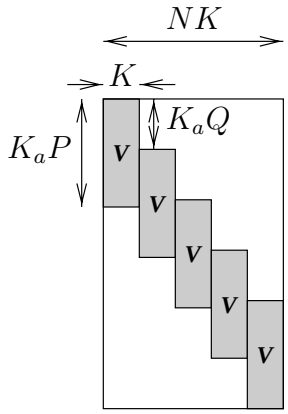

Figure 3: *The structure of $\boldsymbol{T}$. In this example, $N = 5$ and $\lceil P/Q \rceil = 3$.*

III. Diagonalizing Block-Circulant Matrices

The class of Toeplitz matrices is related to circulant matrices [4] and there exists a straightforward and efficient method that can compute the solution of equations involving circulant matrices. This method can be extended to deal with block-circulant matrices. The specific structure of $\boldsymbol{T}$ allows us to successfully apply this method to solve (2).

Circulant Matrices

A circulant matrix is a Toeplitz matrix with the additional restriction that it must be square and each column is a rotated version of the column to the left of it [4]. A block-circulant matrix $\boldsymbol{C}$ of size $DQ \times DK$ with

blocks of size $Q \times K$ thus has the property

$$\boldsymbol{C}_{i,j} = \boldsymbol{C}_{\tilde{i},\tilde{j}} \quad \text{with} \quad \begin{matrix} \tilde{i} = (i+Q) \bmod DQ, \\ \tilde{j} = (j+K) \bmod DK. \end{matrix} \tag{10}$$

Therefore, each element of $\boldsymbol{C}$ has the same value as the element Q rows below and K columns to the right of it. Indices in this calculation that exceed the size of $\boldsymbol{C}$ wrap around and correspond to indices in the first block-row and block-column of $\boldsymbol{C}$.

Systems of equations like

$$\boldsymbol{C}\boldsymbol{x} = \boldsymbol{b}, \tag{11}$$

where $\boldsymbol{C}$ is a circulant matrix with block size 1×1, can be solved efficiently since $\boldsymbol{C}$ can be *diagonalized* with discrete Fourier transforms [7]. In turn, discrete Fourier transforms can be implemented efficiently via *Fast Fourier Transform* (FFT) algorithms. It is an inherent property of circulant matrices that their eigenvectors are the columns of the Fourier transform matrix $\boldsymbol{F}$. This means that we can write every circulant matrix $\boldsymbol{C}$ as [3]

$$\boldsymbol{C} = \boldsymbol{F}^{-1}\boldsymbol{\Lambda}\boldsymbol{F} \tag{12}$$

where $\boldsymbol{\Lambda}$ is a diagonal matrix that contains the eigenvalues of $\boldsymbol{C}$ on its diagonal. Substituting this into (11) yields

$$\boldsymbol{\Lambda}\boldsymbol{F}\boldsymbol{x} = \boldsymbol{F}\boldsymbol{b}. \tag{13}$$

The matrix $\boldsymbol{\Lambda}$ itself can also be computed with a Fourier transform according to

$$\operatorname{diag}(\boldsymbol{\Lambda}) = \boldsymbol{F}\boldsymbol{C}(:,1) \tag{14}$$

where $\operatorname{diag}(\boldsymbol{\Lambda})$ denotes the diagonal elements of $\boldsymbol{\Lambda}$ rearranged as a vector and $\boldsymbol{C}(:,1)$ is the first column of $\boldsymbol{C}$.

We can therefore solve (11) in the frequency domain as long as $\boldsymbol{C}$ is not singular (i. e., it has only non-zero eigenvalues):

$$\boldsymbol{x} = \operatorname{IDFT}(\operatorname{DFT}(\boldsymbol{b})./\operatorname{DFT}(\boldsymbol{C}(:,1))), \tag{15}$$

where $\operatorname{DFT}(\cdot)$ and $\operatorname{IDFT}(\cdot)$ denote the discrete Fourier transform of a vector and its inverse, respectively, and ./ denotes element-wise division.

Block Circulant Matrices

When dealing with block matrices we also need to apply block-Fourier transforms. Suppose $\boldsymbol{C}_{(Q,K)} \in \mathbb{C}^{DQ \times DK}$ is block-circulant with a block size of $Q \times K$. Then we can find a block-diagonal matrix $\boldsymbol{\Lambda}_{(Q,K)}$ with the same block size such that

$$\boldsymbol{C}_{(Q,K)} = \boldsymbol{F}_{(Q)}^{-1}\boldsymbol{\Lambda}_{(Q,K)}\boldsymbol{F}_{(K)} \tag{16}$$

where $\boldsymbol{F}_{(Q)} \in \mathbb{C}^{DQ \times DQ}$ and $\boldsymbol{F}_{(K)} \in \mathbb{C}^{DK \times DK}$ are block-Fourier transforms with a block size of $Q \times Q$ and $K \times K$, respectively. They are defined as

$$\boldsymbol{F}_{(n)} = \boldsymbol{F} \otimes \boldsymbol{I}_n \tag{17}$$

where $\boldsymbol{I}_n$ is the identity matrix of size $n \times n$, $\boldsymbol{F} \in \mathbb{C}^{D \times D}$ and $\otimes$ denotes the Kronecker product.

As before, the matrix $\boldsymbol{\Lambda}_{(Q,K)}$ can be computed with a block-Fourier transform of the first block-column of $\boldsymbol{C}_{(Q,K)}$. Let $\operatorname{diag}_{(Q,K)}(\boldsymbol{\Lambda}_{(Q,K)})$ denote the blocks of size $Q \times K$ on the block-diagonal of $\boldsymbol{\Lambda}_{(Q,K)}$ rearranged as a $DQ \times K$ matrix. Then we have

$$\operatorname{diag}_{(Q,K)}(\boldsymbol{\Lambda}_{(Q,K)}) = \boldsymbol{F}_{(Q)}\boldsymbol{C}_{(Q,K)}(:, 1\!:\!K) \tag{18}$$

where $\boldsymbol{C}_{(Q,K)}(:, 1\!:\!K)$ denotes the first K columns of $\boldsymbol{C}_{(Q,K)}$.

Equation (11) thus reduces to

$$\boldsymbol{\Lambda}_{(Q,K)}\boldsymbol{F}_{(K)}\boldsymbol{x} = \boldsymbol{F}_{(Q)}\boldsymbol{b}. \tag{19}$$

The block-Fourier transforms denoted by $\boldsymbol{F}_{(Q)}$ (and $\boldsymbol{F}_{(K)}$) and their inverses can be performed with Q (K) non-block discrete (inverse) Fourier transforms of length D. Next we have to invert $\boldsymbol{\Lambda}_{(Q,K)}$. Since the blocks on the diagonal of $\boldsymbol{\Lambda}_{(Q,K)}$ are essentially unstructured, this can, for example, be achieved by some standard method like the Cholesky decomposition of $\boldsymbol{T}^H\boldsymbol{T}$ and two back-substitutions.

IV. Application to TD-CDMA

Although $\boldsymbol{T}$ in (2) is not block-square, the

block-columns of $\boldsymbol{T}$ are already rotated versions of the first block-column. Therefore, we can simply add block columns to it until it is block-square. The number of block-columns that we must add depends on the degree of the block-band structure of $\boldsymbol{T}$, which is the same as the inter-symbol interference in the original transmission system. Figure 4 continues figure 3 and shows how $\boldsymbol{T}$ can be extended to be block-circulant.

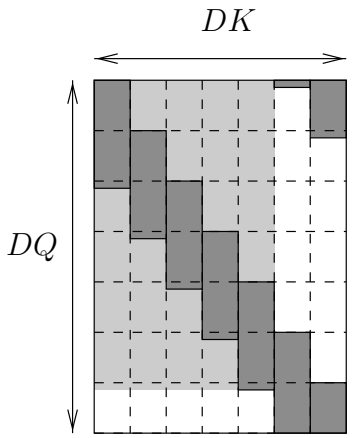

Figure 4: *Making $\boldsymbol{T}$ (light shaded part) block-circulant.*

After $\boldsymbol{T}$ has been extended to be block-circulant, it has $D \times D$ blocks of size $Q \times K$, where $D = N + \lceil P/Q \rceil - 1$.[1] The vector $\boldsymbol{e}$ needs to be zero-padded at its end so that it has length DQ. Likewise, the new solution vector contains the desired results in its first NK elements.

Simulations (figure 7) have shown that the error made by solving for $\boldsymbol{d}$ with this extended version of $\boldsymbol{T}$ is insignificant. This is due to the fact the the distortions introduced by making $\boldsymbol{T}$ block-square affect mainly the guard periods between bursts.

V. Overlap-Save

The convolution matrix $\boldsymbol{T}$ with its strong band structure offers possibilities to reduce the computational demands of the joint detector even further. Just as it is possible to perform the convolution of a long signal with a much shorter filter impulse response with the well known overlap-save technique [5], it is possible to use this technique for equalizing such a filter.

The idea is to reduce the size of the involved matrices and solve the whole problem by solving multiple smaller ones instead. The reduction in size is expressed by forcing D to smaller values when deriving a block-circular matrix from $\boldsymbol{T}$ according to figure 4. With such a smaller matrix only a smaller part of the data vector can be estimated of course; thus, we need to partition the data vector into slices of length D. But if D is smaller than its ideal value $N + \lceil P/Q \rceil - 1$, the distortions mentioned in the previous section do no longer fall into the guard period, leading to unacceptable errors in the estimated data vector slices.

Figure 5 depicts this effect. The dashed line shows the relative error of the data symbols of one user where D has been set to 32 and the full vector of $N = 69$ symbols has been calculated by carrying out the frequency domain detection three times on successive blocks of 32 symbols each. Obviously, each run of $D = 32$ symbols has large errors at the beginning and the end, but not in its middle part.

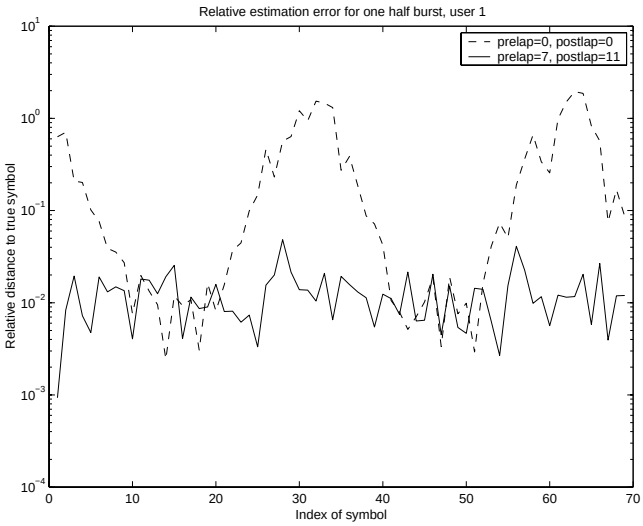

Figure 5: *Estimation errors when using overlap-save techniques. $Q = 16$, $W = 57$, $N = 69$, $K = 4$, $D = 32$, no noise.*

As a remedy, one discards a certain num-

[1] The notation $\lceil x \rceil$ denotes the *ceiling* of x, i. e., the smallest integer that is greater than or equal to x.

ber of symbols at the start of the data vector slice (the *prelap*) and at the end of it (the *postlap*). The computation of the complete data vector needs to be arranged in such a way that the discarded symbols from the previous slice can be found in the middle of the next one as depicted in figure 6. Figure 5 also shows that the relative error for such an overlapping computation has been reduced to a lower level for all symbols (solid line).

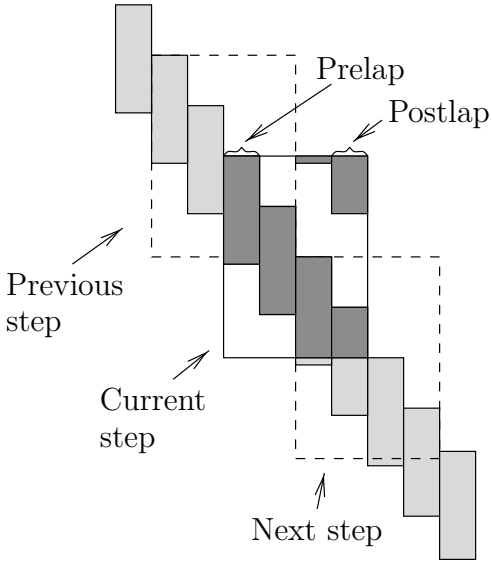

Figure 6: *Overlapping Convolution Matrices*

VI. Simulation Results and Computational Complexity

Figure 7 compares the frequency domain approach for different overlapping degrees with the true least squares solution, obtained via a Cholesky factorization of $\boldsymbol{T}^H\boldsymbol{T}$. For white noise, the least squares solution corresponds to the zero forcing block linear equalizer. As expected, the bit error ratio performance of the frequency domain approach is closest to the true least squares solution if no overlap-save has been employed. The simulation results also verify that using more overlap leads to a better performance. The figure also shows the performance of a joint detector that uses an approximate Cholesky decomposition [8]. The simulations for the approximated Cholesky joint detector have been carried out by using a row-oriented approximation method that computes only the first five block-rows.

The simulation scenario includes $K = 4$ users. To investigate the near/far resistance of the joint detector, two of these users have a power that is 20 dB above the remaining two users. This corresponds to a severe near/far scenario. The bit error ratio shown in figure 7 is the mean of the two weaker users. It shows that the presented joint detector is able to handle this critical situation better than the approximated Cholesky joint detector. The receiver has $K_a = 1$ antenna.

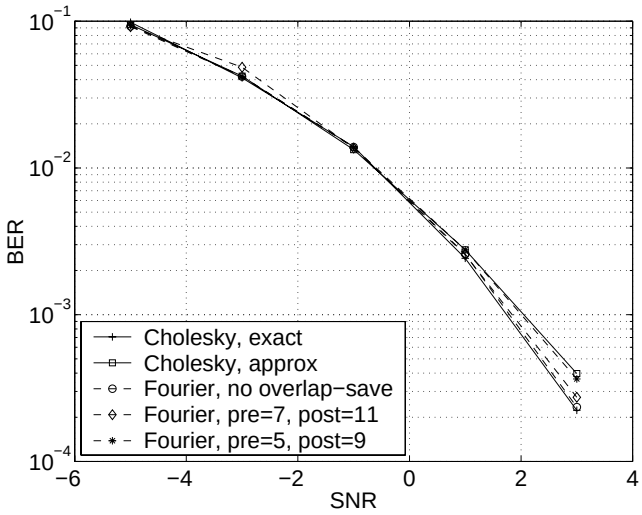

Figure 7: *Bit error ratios of joint detection using Fourier transformations vs. Cholesky decomposition.* $Q = 16$, $W = 57$, $N = 69$, $K = 4$, $D = 32$, $K_a = 1$.

Figures 8 and 9 compare the computational complexity of the joint detection algorithms that have been used in the simulations of figure 7. It can be seen that the frequency domain approach has a lower computational complexity than the approcimated Cholesky approach.

VII. Conclusions

In this paper, we have shown that performing joint detection in the frequency domain has a lower computational complexity

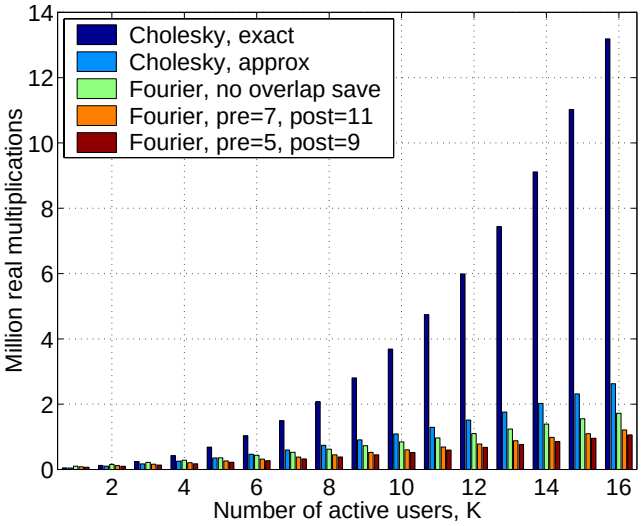

Figure 8: *Computational complexity of the joint detection algorithms, put against the number of active codes,* K. $Q = 16$, $W = 57$, $N = 69$, $D = 32$, $K_a = 1$.

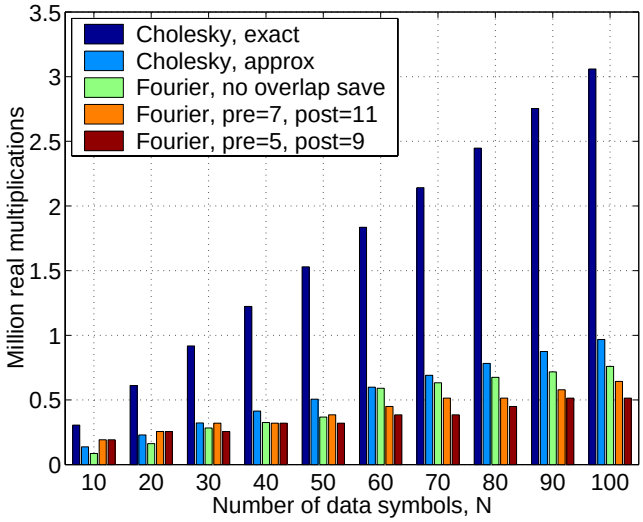

Figure 9: *Computational complexity of the joint detection algorithms, put against the number of data symbols,* N. $Q = 16$, $W = 57$, $K = 8$, $D = 32$, $K_a = 1$.

than the approximated Cholesky joint detector while delivering a better bit-error ratio performance. The low computational complexity has been achieved by using overlap-save techniques for the deconvolution. Overlapping was performed both at the beginning and at the end of the considered data vector.

Both the block-FFTs and the inversion of the diagonalized system matrix consist of independent subproblems that can be solved in parallel.

References

[1] G. Ammar and W.B. Gragg. Superfast Solution of Real Positive Definite Toeplitz Systems. *SIAM J. Matrix Anal. Appl.*, 9:61–76, 1988.

[2] J. Blanz, A. Klein, M. Naßhan, and A. Steil. Performance of a Cellular Hybrid C/TDMA Mobile Radio System Applying Joint Detection and Coherent Receiver Antenna Diversity. *IEEE Journal on Selected Areas in Communications*, 12(4), May 1994.

[3] L. Eldén and E. Sjöström. Fast computation of the principle singular vectors of Toeplitz matrices arising in exponential data modelling. *Signal Processing*, 50(1-2):151–164, April 1996.

[4] G.H. Golub and C.F. van Loan. *Matrix Computations*. The John Hopkins University Press, third edition, 1996.

[5] S. Haykin. *Adaptive Filter Theory*. Prentice Hall, third edition, 1996.

[6] P. Jung and J. J. Blanz. Joint detection with coherent receiver antenna diversity in CDMA mobile radio systems. *IEEE Trans. on Vehicular Technology*, 44:76–88, 1995.

[7] C.F. Van Loan. *Computational Frameworks for the Fast Fourier Transform*. SIAM Publications, Philadelphia, PA, 1992.

[8] J. Mayer, J. Schlee, and T. Weber. Realtime feasibility of joint detection CDMA. In *Proc. 2nd European Personal Mobile Communications Conference*, pages 245–252, Bonn, Germany, September 1997.

[9] M. Vollmer, M. Haardt, and J. Götze. Exploiting the structure of the joint detection problem with decision feedback. In *Proc. 3rd European Personal Mobile Communications Conference (EPMCC)*, Paris, France, March 1999.